Field-Flow Fractionation: Addressing the Nano Challenge

ARTICLE *in* ANALYTICAL CHEMISTRY · NOVEMBER 2010

Impact Factor: 5.64 · DOI: 10.1021/ac101759z · Source: PubMed

3 AUTHORS, INCLUDING:

J. Ray Runyon
SOLVE Research and Consultancy, AB
11 PUBLICATIONS **187** CITATIONS
SEE PROFILE

Akram Ashames
Colorado School of Mines
1 PUBLICATION **42** CITATIONS
SEE PROFILE

analytical chemistry

FEATURE

pubs.acs.org/ac

Field-Flow Fractionation: Addressing the Nano Challenge

Field-flow fractionation is coming of age as a family of analytical methods for separating and characterizing macromolecules, nanoparticles, and particulates. The capabilities and versatility of these techniques are discussed in light of the challenges that are being addressed in analyzing nanometer-sized sample components and the insights gained through their use in applications ranging from materials science to biology. (To listen to a podcast about this feature, please go to the *Analytical Chemistry* multimedia page at pubs.acs.org/page/ancham/audio/index.html.)

S. Kim Ratanathanawongs Williams, J. Ray Runyon, and Akram A. Ashames

Colorado School of Mines

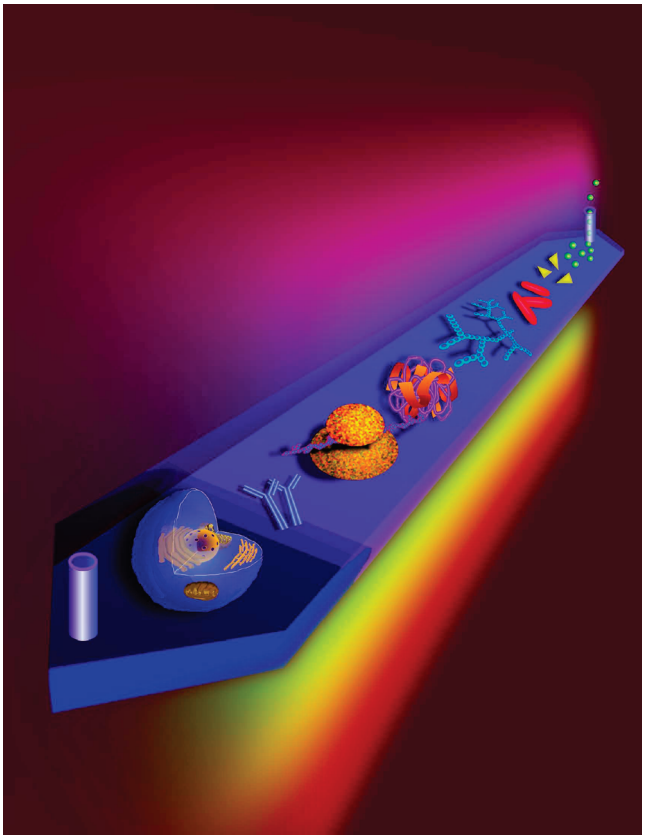

Robert Gates

In 1966, the late J. Calvin Giddings introduced field-flow fractionation (FFF), a chromatography-like technique with an essentially one-phase nature that gives it a potential advantage in separating macromolecules and colloids.[1] The ensuing years brought tremendous innovations in instrumentation that utilized different types of fields, advances in understanding the behavior of these large analytes in laminar flow streams in confined channels, and numerous applications that demonstrated the versatility of FFF. However, as recently as the mid-1990s, FFF was still described as an interesting technique looking for a niche.

Research in fields such as nanoscience and nanotechnology and biotechnology subsequently exploded. It is recognized that these nanometer-sized analytes are usually not monodispersed and in fact can undergo dynamic interactions that cause quantitative shifts in subpopulations. New metrologies and analytical methods to investigate properties and validate theoretical and behavioral models in this size regime were urgently needed.

As the "nano" revolution unfolds, challenges arise from the diverse primary and secondary properties such as size, shape, architecture, composition, optical and electronic properties, and toxicity of nanoparticles, polymers, and nanocomposites. Regulatory agencies are considering more rigorous monitoring of aggregates in protein-based pharmaceuticals and vaccines because of concerns about reduced efficacies and potential immunogenic responses. Many questions about the function of subcellular components that were previously disregarded have become the focus of attention; some of these components are also potential disease biomarkers. Separating these complex and polydisperse samples into simpler units for further analysis and testing is key in gaining detailed insights that would otherwise be unachievable.

FFF is a family of techniques that was designed to separate and measure physicochemical properties of complex macromolecular, colloidal, and particulate materials.[1−3] The separation occurs by differential displacement in a flowing stream of liquid that carries the separated components to a detector. Physicochemical properties of the species determine the measured retention time, t_r, and thus characterization is usually achieved simultaneously with separation. The easy elution and collection of highly uniform sample components from the channel outlet is a major strength of FFF techniques. Each fraction can be examined either using offline techniques or online methods such as light scattering, MS, and element specific detectors to obtain complementary information about different types of distributions. The separation mechanism and open parallel plate FFF channel design results in other important characteristics such as low shear rates (ideal for investigating fragile species), low sample loss, tunable selectivity and speed, applicability to diverse samples spanning a broad molecular weight/size range, and ability to separate according to different physicochemical properties.

Published: November 19, 2010

dx.doi.org/10.1021/ac101759z | *Anal. Chem.* 2011, 83, 634–642

The goals of this article are to briefly revisit the basic principles of FFF; demonstrate the strengths of the FFF family of techniques and how they have been used to address analytical challenges encountered with nanometer-sized analyte species and complex samples; highlight recent advances in FFF instrumentation including the importance of hyphenated methods; and increase the awareness of researchers who may benefit from FFF's many capabilities for analyzing macromolecules and nanoparticles. ("Nano" is commonly used in reference to matter with dimensions ~1−100 nm that exhibit unique phenomena.[4] The authors have included macromolecules in this discussion because they are often in the nanometer size range.)

BASIC PRINCIPLES

FFF separation is an essential step in meeting the nano challenge because many samples possess continuous distributions in one or more properties and/or consist of multiple components that span a wide size or molecular weight range. FFF takes place in a thin, ribbon-like channel in which a laminar flow with a parabolic flow velocity profile is subjected to a perpendicularly applied external field.[2] The underlying principle of all FFF techniques is based on the balance between field-induced mass transport of analyte towards an accumulation wall and diffusion away from this wall caused by the resulting concentration gradient. This leads to the formation of sample clouds which, at steady state, have equilibrium mean layer thicknesses $\ell_1, \ell_2, \ldots$ etc. with different ℓ values corresponding to different flow velocity streamlines of the parabolic flow profile and thus different t_r. Ideally, each sample component has a unique ℓ or $D/|U|$ where D is the diffusion coefficient and U is the field-induced migration. The smaller the D and/or the larger the interaction with the field, the smaller the ℓ value and the longer the sample component remains in the FFF channel. The relationship between ℓ, t_r, and the force, F, exerted on a single particle or macromolecule by the applied field can be approximated by the equation[2,3]

$$\frac{t_r}{t^0} = \frac{w}{6\ell} = \frac{|F|w}{6kT} \tag{1}$$

where t^0 is the void time, w is the channel thickness, k is Boltzmann's constant, and T is absolute temperature. The assumptions are that all particles are noninteracting point masses and $w \gg \ell$ (necessary for efficient separation). The above equation shows that F governs both retention and separation because differences in the force experienced by various particles, ΔF, will result in roughly proportional differences in t_r. The magnitude of F and ΔF depends on particle properties, field strength, and the type of field employed.

Virtually any type of field can be used as long as it interacts with some physicochemical property of the sample components to drive them to the accumulation wall. This has given rise to multiple techniques within the FFF family, many of which have yet to be commercialized, e.g., dielectrophoretic, magnetic, electrical, and acoustic.[5−8] Thermal, sedimentation, and crossflow FFF are commercially available and are thus the most commonly used FFF techniques.

Thermal FFF (ThFFF). This first experimentally realized FFF technique utilizes a temperature gradient to drive samples to the accumulation wall.[9] The ribbon-like channel is sandwiched between two heat conductive blocks that are individually temperature controlled, one with heating elements and the other with circulating chilled water or coolant. Temperature differences between the hot and cold walls can be as high as ~100 K, which when applied across the channel thickness of $\sim 10^{-2}$ cm, translates to gradients that are $\sim 10^4$ K cm^{-1}. ThFFF was originally used for synthetic polymers in organic solvents but has been expanded to nanoparticles in aqueous and nonaqueous solvents.[10,11] The effective driving force on each polymer molecule is

$$F = kT \frac{D_T}{D} \frac{dT}{dx} \tag{2}$$

where D_T is the thermal diffusion coefficient and dT/dx is the applied temperature gradient. Combining Equations 1 and 2 reveals that t_r is proportional to the field strength (dT/dx) and the Soret coefficient, D_T/D, and that the measurement of t_r yields D_T/D. If D_T is known, D can be calculated, which subsequently yields molecular weight MW because of the dependence $D \cong A(MW)^{-b}$ where A is an experimentally determined proportionality constant and b is ~0.6 for a thermodynamically favorable solvent. Alternatively, if D is known, D_T can be calculated. ThFFF is one of the most intriguing techniques of the FFF family because the D_T term can be used to address analytical challenges associated with polymer and nanoparticle interfacial composition and polymer microstructure and architecture.[12] However, retention times are difficult to calculate because thermal diffusion in liquids is not fully understood and D_T values specific to the particular polymer and nanoparticle are not widely available. This situation is being remedied by coupling ThFFF to detectors that measure MW independently and by ongoing efforts to evaluate existing theories for predicting D_T.[13]

Sedimentation FFF (SdFFF). The FFF channel encircles a spinning centrifuge basket that generates differential acceleration forces on different particles.[14] The force experienced by a particle can be written in various forms to show the relationship between the field strength (or acceleration, G) and the effective mass (true mass minus buoyant mass), m', particle volume, V_p, diameter, d, and the difference in density between the particle and carrier liquid, $\Delta\rho$.

$$F = m'G = V_p|\Delta\rho|G = \frac{\pi}{6} d^3|\Delta\rho|G \tag{3}$$

Substituting F into Equation 1 yields a proportionality between t_r and d^3 that explains SdFFF's ability to baseline resolve particle aggregates ranging from singlets to octuplets.[15] A 10× difference in d will yield a 1000× difference in t_r or a diameter-based selectivity (defined as $|d \log t_r / d \log d|$) of 3. Though this level of selectivity is highly desirable in certain situations, analyses for polydisperse samples are lengthy. This is readily resolved by decreasing the field strength according to a theoretical function that maintains a constant fractionating power throughout the separation.[3] The proportionality between t_r and m' is also important because it allows SdFFF to be used as a microbalance for measuring minute $(10^{-16}-10^{-18}$ g) changes in nanoparticle effective mass.[16,17]

Crossflow FFF (FlFFF). Crossflow or flow FFF is the most commonly used FFF technique. A crossflow of fluid transports the sample to the accumulation wall which, in this case, is a semipermeable membrane laid over a supporting frit panel.[18] Theoretical calculations have confirmed that the typical FlFFF crossflow flow rates do not perturb the parabolic flow profile.[19] In theory, FlFFF is universally applicable to all analyte species. In practice, the lower size limit is set by the molecular weight- or size- cutoff of the membrane, which determines not only the

dx.doi.org/10.1021/ac101759z |Anal. Chem. 2011, 83, 634–642

analyte species retained in the channel, but also the highest crossflow rates that can be used. The driving force exerted on a single particle is related to the friction coefficient, f, viscosity, η, and the Stokes or hydrodynamic diameter, d, by the following series of equations:

$$F = f|U| = kT\frac{|U|}{D} = 3\pi\eta|U|d \quad (4)$$

where U is synonymous with crossflow velocity. This equation (and Equation 1) shows that t_r is dependent on the analyte's diffusion coefficient, which in turn is related to a sphere equivalent hydrodynamic d. Assuming all particles in the sample are similar in shape, qualitative interpretation of the measured fractogram is straightforward because t_r is proportional to d and the fractogram reflects the size distribution. Different variants of the FlFFF channel design include the original symmetric channel with two permeable walls, today's most commonly used asymmetric channel with one non-permeable wall (AsFlFFF, also known as AF4),[20] and the hollow fiber channel.[21] Unlike ThFFF and SdFFF channels, which are constructed from rugged metallic materials, the relatively delicate membrane accumulation wall in FlFFF channels requires careful treatment and periodic replacement.

Dielectrophoretic FFF (DEP-FFF). Dielectrophoresis is the migration of a particle in a non-uniform electric field caused by electrostatic interactions between the field-induced polarization in the particle and the field.[5,22] The DEP force experienced by a spherical particle of radius r is related to the permittivity (or dielectric constant) of the medium, ε_s, and the imposed inhomogeneous electric field, $\vec{E}$.

$$F = 2\pi r^3 \varepsilon_s f_{cm} \vec{\Delta} \,|\, \vec{E}|^2 \quad (5)$$

The Clausius-Mossotti factor, f_{cm}, takes into account complex permittivities of the particle and the suspending medium and determines the relative strength and direction of the DEP force on a particle as a function of the applied field frequency. Hence, particles can be separated in a DEP-FFF system on the basis of differences in effective dielectric properties, such as semiconductor particle bandgaps and electronic characteristics.[23] DEP forces also depend on the spatial distribution of the applied electrical field, and advances in microfabrication technologies have enabled the production of interdigitated microelectrode arrays capable of producing large DEP forces with small applied voltages.[5,22]

Magnetic FFF (MgFFF). Various MgFFF instrument configurations have achieved varying degrees of success. The most recent is a quadrupole MgFFF (QMgFFF) instrument comprised of a helical separation channel mounted in an axisymmetric magnetic field.[6] The outwardly radial magnetic field sets up a field gradient across the channel, and the magnitude of the gradient's interaction with the magnetic component of the particles determines t_r. The force experienced by a single particle under the influence of the magnetic field gradient is given by

$$F = V_m M|\nabla B| \quad (6)$$

where V_m is the volume of the magnetized component of the particle, M is the magnetization of this component (which is related to magnetic susceptibility), and ∇B is the gradient in magnetic field B.

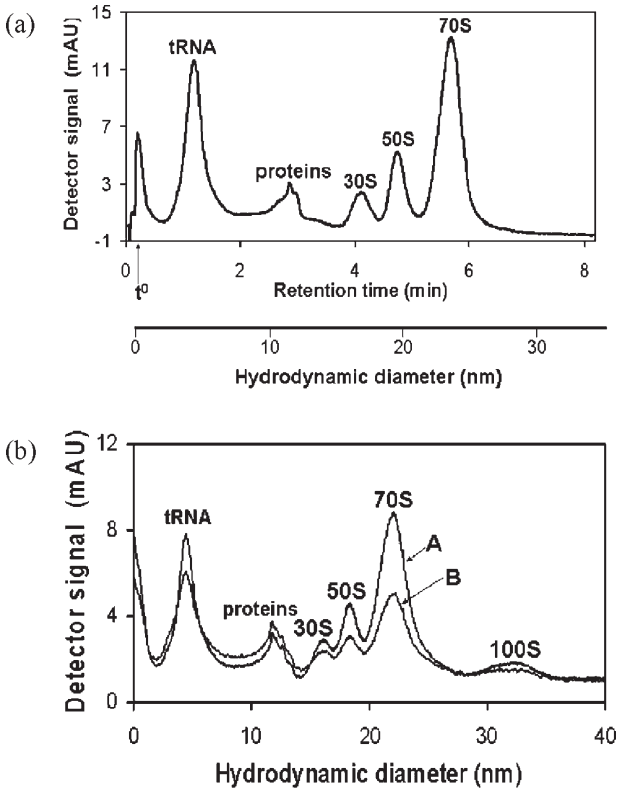

Figure 1. AsFlFFF analysis of ribosomal samples taken in (a) the exponential bacterial growth phase and (b) 5 h after inoculation in the midexponential phase. The two traces in (b) represent absorbance at λ = 260 nm (A) and 280 nm (B). Reprinted from ref 24 with permission from Elsevier.

Summary. Equations 1−6 describe the normal mode separation mechanism that analytes smaller than ~1 μm experience and explain why small (high diffusion coefficient) analytes elute first. For analytes >~1 μm, the steric-hyperlayer separation mechanism reverses elution order,[3] but this Feature focuses on nano-sized materials, which are usually separated by the normal mode.

These six equations also provide insight into experimental parameters and sample properties that govern retention, the properties by which the sample components can be sorted into a series of more uniform bins, and the information that can be garnered using each type of field. Moreover, the elution profile or fractogram can be transformed into distributions specific to the field that was employed, e.g., size distributions for FlFFF or mass or density distributions for SdFFF. Increasingly, FFF coupled with orthogonal methods provides complementary information and thus a more complete picture of sample characteristics. This next section demonstrates the important features of FFF, drawing on examples that include macromolecules and nanoparticles.

FFF SEPARATION AND ANALYSIS

Selectivity and Complex Samples. FFF techniques separate analytes according to different properties depending on the field applied. The selectivity of the separation depends on the relationship between retention time and the specific sample property being probed. For example, because $t_r \propto d^3$ for SdFFF and $t_r \propto d$ for FlFFF, the diameter-based selectivities are 3 and 1, respectively. The higher the selectivity, the smaller the difference in size

dx.doi.org/10.1021/ac101759z |Anal. Chem. 2011, 83, 634–642

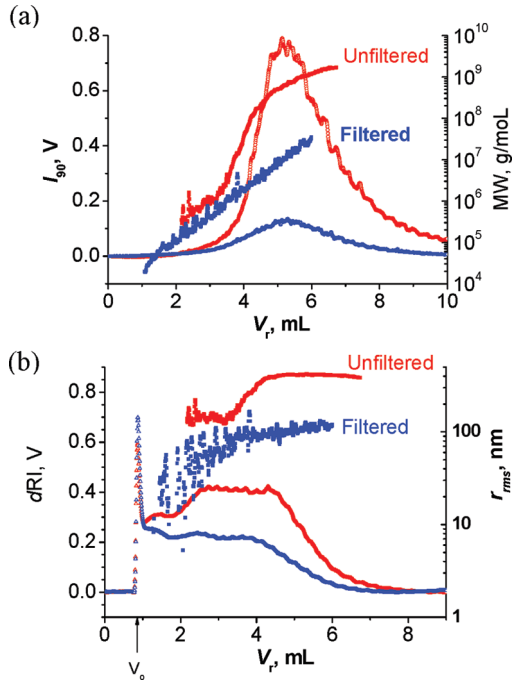

Figure 2. ThFFF-MALS analysis of ultrahigh *MW* PVAc. (a) MALS fractogram and *MW*s and (b) dRI fractogram and r_{rms} of unfiltered (red) and filtered (blue) PVAc. (I_{90}: light scattering intensity at 90°; V_r: retention volume). Reprinted from ref 26 with permission from Elsevier.

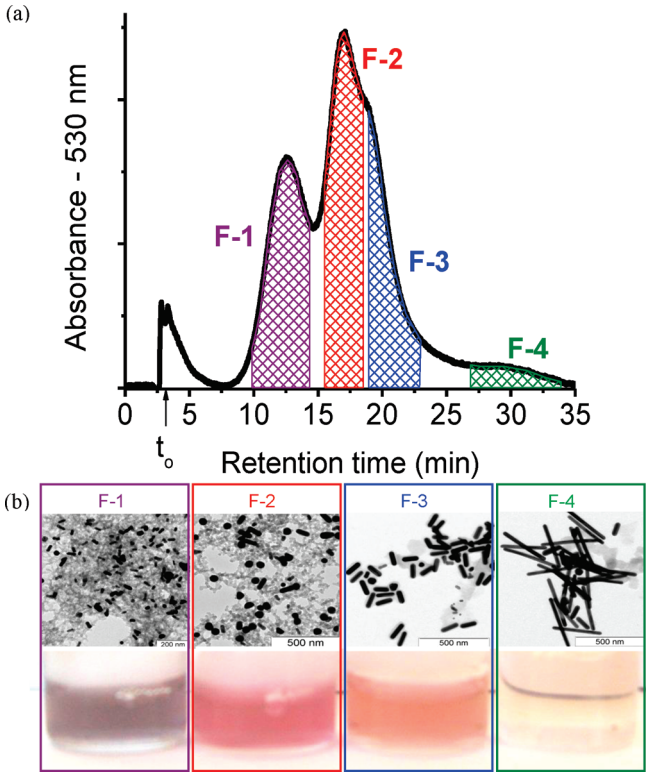

Figure 3. (a) AsFlFFF fractogram of GNRs. The cross-hatched regions designate retention times of four different collected fractions. (b) TEM images and associated solution colors of collected fractions.

that can be differentiated by retention time. This is the figure of merit in the separation of polydisperse samples because the continuous distributions in size, mass, etc. are expected to produce broad elution profiles. Different components elute at different times even though distinct peaks are not evident. Hence, the traditional metric of number of theoretical plates is not as useful for describing the effectiveness of the separation of non-uniform nano-sized materials.

The main challenges in biotechnology are understanding growth properties of cell cultures and optimizing protein yields. For example, the total amount of ribosomal material per cell and the relative amount of the assembled 70S ribosome are indicators of the cells' protein translation capacity. Thus, separation and quantitation of types of ribosomal material can provide invaluable insights for establishing optimum bioreactor conditions. Figure 1 demonstrates the level of resolution obtained by AsFlFFF in the low nanometer size region in a complex ribosomal sample.[24] The AsFlFFF fractograms show that the 30S and 50S ribosomal subunits (~16 and 18 nm) and 70S assembled unit (~25 nm) are clearly resolved and separated from tRNA and proteins within 8 min. The analysis time was optimized so that a sample can be withdrawn from the bioreactor, processed, and analyzed in 16 min cycles. The advantage of a separation step over simply measuring the average size of components in the entire sample is clearly demonstrated by Figure 1b. The fractogram from a sample collected at the mid-exponential growth phase shows a peak that is believed to be 100S ribosomal particles, a component that would have been missed if only the average diameter was measured. Similar separations are obtainable for nanoparticles.[25]

Wide Molecular Weight and Size Range. Samples are routinely filtered prior to chromatographic separations, and the columns themselves have built-in frits to remove large sample components that can be deleterious to column performance. Because FFF channels are open structures with typical thicknesses of ~100−500 μm, oftentimes the entire sample can be analyzed without filtration. Figure 2 shows ThFFF fractograms for filtered and unfiltered poly(vinyl acetate) (PVAc) samples and their (a) *MW* and (b) root mean square radius, r_{rms}, obtained by online multiangle light scattering-differential refractive index (MALS-dRI) detection.[26] This detector combination confirms the success of a separation that spans five orders of magnitude in *MW* and at r_{rms} values up to 400 nm. The low shear rates encountered in FFF channels significantly reduce the possibility for shear degradation of ultrahigh *MW* polymers. The dRI plot in Figure 2b reveals that filtration unexpectedly removes a significant amount of lower *MW* soluble polymers, which leads to erroneous results. This study demonstrated that the routine sample filtration used as a standard step in many macromolecular analyses must be performed judiciously.

Size Separation. Size and size distributions play important roles in optical and electrical properties, fate and transport, and biological efficacy. FFF has been used to characterize a wide variety of nanoscale materials, including engineered nanoparticles (quantum dots,[25,27,28] fullerenes,[29] and carbon nanotubes[30]); environmental colloids;[31−33] natural and synthetic macromolecules;[26,34−37] proteins, protein aggregates, and protein virus-like particles;[38−44] drug and gene therapy delivery vehicles;[45−47] and subcellular particles.[24]

Nanoparticle shape has dramatic effects on optical properties. For example, gold nanorods (GNRs) have been proposed for applications such as bioimaging and biosensing because different aspect ratios of the rods will have characteristic absorbance wavelengths that can be discerned in a multiplexed analysis. The use of FFF to achieve what is effectively a shape-based separation of

dx.doi.org/10.1021/ac101759z |*Anal. Chem.* 2011, 83, 634–642

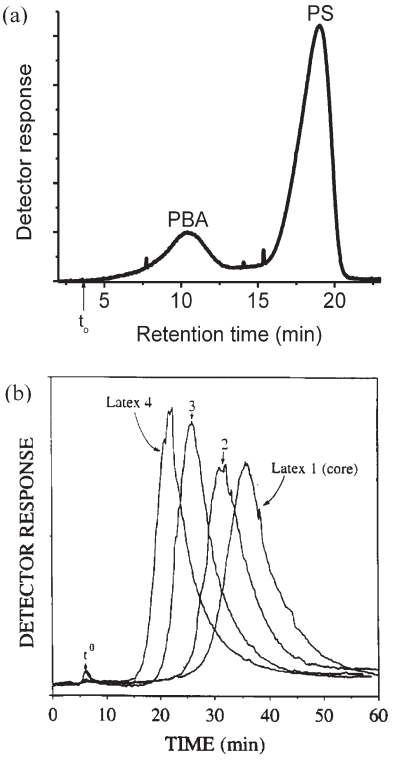

Figure 4. Composition-based ThFFF separations. (a) PS and PBA polymers with similar hydrodynamic radii. (b) Core-shell nanoparticles with different PBA:PMAA shell compositions. Latex 1: 135 nm PS core; Latex 2: 9% PMAA shell; Latex 3: 15% PMAA shell; Latex 4: 36% PMAA shell. Part b reprinted from ref 10 with permission from Elsevier.

a polydisperse GNR sample is shown in Figure 3. Fractions F1−F4 were collected at the indicated time intervals in Figure 3a and contained GNR subpopulations of increasing length as evidenced by transmission electron microscopy (TEM) images in Figure 3b. A suspension of each fraction is shown below its corresponding TEM image; the different colors further confirm the presence of different GNR subpopulations.[48] This GNR separation is based on the sphere equivalent hydrodynamic diameter as described by Equation 4. Though this is not a true shape separation, this example demonstrates the possibility of obtaining fractions containing different aspect ratio nanoparticles. FlFFF-MALS has also been successfully used to separate and characterize DNA stabilized single walled nanotubes in an aqueous carrier liquid according to length.[30]

Mass. Functionalized nanoparticles are used in many applications ranging from immunodiagnostics to reinforced plastics. The ability to quantitate the amount of (physically or chemically) attached functionalities can provide insights into the behavior and performance of these nanoparticles. SdFFF is well suited for this task because t_r is proportional to m' of the particle (Equation 3). Hence, the adsorption or attachment of proteins, polymers, or other functionalities to the surface of nanoparticles is reflected by an increase in t_r. SdFFF has been used as a microbalance for measuring minute (10^{-16}−10^{-18} g) changes in m' and monitoring different stages in the development of a nanoparticle-based bioluminescent immunosensor.[17] This biosensor, which has a detection limit of 15 fmol, consisted of polystyrene (PS) latex particles that were first coated with a surfactant and then with bovine serum albumin (BSA). SdFFF measurements yielded a saturation level loading of 700 nmol pyruvate kinase-IgY (antiBSA) conjugate per 7.5×10^{10} BSA coated particles and an average of 22 BSA molecules per pyruvate kinase-IgY conjugate.

Composition. Elasticity, adhesiveness, haziness, and phase separation behavior are examples of polymer properties that depend on composition. ThFFF can separate organosoluble macromolecules by composition, despite an incomplete understanding of thermal diffusion. Figure 4a shows a baseline resolved composition separation of PS and poly(*n*-butyl acrylate) (PBA) polymers with similar hydrodynamic radii, r_h, (12.75 nm) and D (4.0×10^{-7} cm^2 sec^{-1}). ThFFF has also been used to separate nanoparticles with different surface compositions. Figure 4b shows the superimposed fractograms of four core−shell latex particles consisting of a 135 nm PS core and shells with varying ratios of PBA and poly(methacrylic acid) (PMAA).[10] The nanoparticle with the largest shell ratio of PBA/PMAA had the shortest retention time, whereas the PS core (smallest particle) was retained longest, suggesting a surface composition dependent retention.

D_T is a unique property of the polymer-solvent pair and varies linearly with copolymer composition. Therefore, ThFFF can determine the copolymer composition of an unknown sample from measured t_r and D.[49] The same has been demonstrated for the core-shell nanoparticles mentioned above.[10]

Band Gap. Carbon nanotubes have been proposed for applications such as high strength and conductive composites, sensors, field emission displays, and hydrogen storage media. Their semiconductive and optical properties depend on their chirality and physical dimensions.[30] Dielectrophoretic forces have been used to separate single wall nanotubes (SWNTs) according to electronic type and to produce fractions that are enriched in different SWNT diameters.[23] Differences in dielectric constants form the basis for these DEP-FFF separations. Because the dielectric constant is governed by the band gap which, in turn, is inversely proportional to diameter, separations based on band gaps and diameter are possible. The former was achieved by utilizing electric field conditions that preferentially trapped metallic species on the electrode while the semiconductor species flowed through the DEP-FFF channel. In the latter case, the enrichment of semiconductor SWNTs of different diameters was achieved by the usual FFF separation mechanism. That is, differences in dielectrophoretic forces caused SWNTs to reside in different flow velocity streamlines in the DEP-FFF channel and elute at different times. Fluorescence and Raman spectra were collected as supporting evidence of separation and enrichment.

Magnetic Susceptibility. The large surface area of magnetic nanoparticles make them attractive candidates for applications such as drug targeting, catalysis, and bioseparation.[6] The synthesis of monodisperse magnetic nanoparticles is difficult to achieve, yet required for medical applications. For instance, to minimize the unwanted systemic effects of pharmaceutical magnetic nanoparticles and allow the use of higher and effective drug doses, the weakly magnetic fraction must be depleted from the polydisperse formulation. There was no method to measure the polydispersity in the magnetic properties of these pharmaceutical nanocarriers until recently, when QMgFFF successfully differentiated three different lots of magnetic nanoparticles[6] and fractionated polydisperse samples of dextran-coated magnetite nanoparticles according to their magnetic susceptibility.

■ COMPLEX SAMPLES AND PROCESSES

High selectivity, wide size range, and low shear rates make FFF ideally suited for the separation of complex and often fragile

dx.doi.org/10.1021/ac101759z |*Anal. Chem.* 2011, 83, 634–642

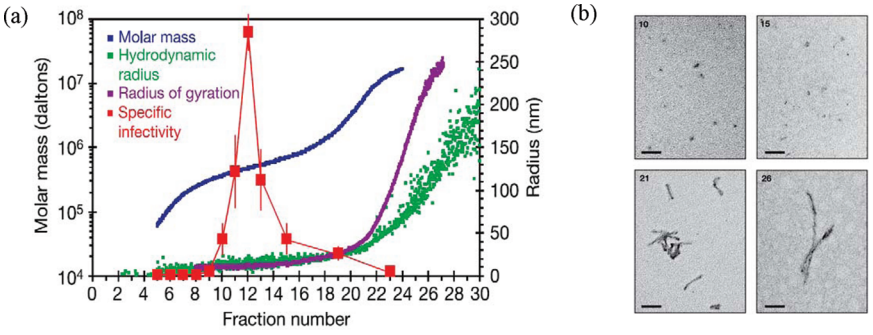

Figure 5. AsFlFFF fractionation and characterization of protease-resistant prion protein particles (PrP^{res}) with online MALS, dRI, and QELS. (a) Specific infectivity of each fraction overlaid with the corresponding molar mass (i.e., molecular weight, *MW*), r_{rms} (i.e., radius of gyration), and hydrodynamic radius (r_h). (b) TEM images of four fractions showing an increase in size and fibril length corresponding to increasing fraction numbers (scale bars = 100 nm). Reprinted from ref 40 with permission from Nature Publishing Group.

samples. Biological and environmental samples tend to be highly complex with multiple components composed of wide arrays of physicochemical properties that can undergo dynamic changes. (The ribosome data shown in Figure 1 is a good example of a complex sample whose components can shift with growth conditions and time.) Thus, it is not surprising that FFF (particularly, FlFFF) has found a niche in these areas.[38−47]

Protein Aggregation. Misfolded and partially unfolded proteins can lead to the formation of aggregates and deposits such as the fibrils and plaques associated with neurodegenerative diseases. Protein aggregates caused by chemical- or physical-induced instabilities during manufacturing, storage, and/or administration can also be present in biotherapeutic products. The link between protein aggregates and immunogenicity, the difficulty of establishing cause-and-effect, and the need for an appropriate suite of instrumentation for analyzing ≤ 10 μm aggregates are currently topics of discussion in this field.[50−52] Key challenges to the characterization of protein aggregates in protein therapeutics include quantitation and identification of aggregates with a wide size range of 0.1−10 μm. An optimized AsFlFFF-MALS-UV method was developed that covered the 50−500 nm size range.[39] Protein self-association attributed to the AsFlFFF sample focusing step was avoided by using moderate flow rates. Quantifying minor species, e.g., high order aggregates, remains an unresolved problem but could be addressed with more sensitive detectors.

A study of a therapeutic immunoglobulin further illustrates the complexity of aggregate-containing samples.[38] A host of analytical methods including AsFlFFF and fluorescence microscopy showed that different types of aggregates can form through non-covalent bonds (e.g., hydrogen bonding, electrostatic repulsion and attraction, and hydrophobic interactions). The flexibility in the choice of FFF carrier liquid was an advantage because amino acid- or formulation-based buffers could be used.

Pathologically, protein aggregation is associated with diseases such as Alzheimer's, Parkinson's, and transmissible spongiform encephalopathies. In a groundbreaking study, AsFlFFF with MALS-dRI-quasielastic light scattering (QELS) detection was essential in demonstrating that aggregates of the protease-resistant prion protein (PrP^{res}) with *MW* of 300−600 kDa, hydrodynamic radius r_h of 14−28 nm, and that are composed of 14−28 PrP^{res} molecules possessed the greatest infectivity (Figure 5a).[40] TEM analysis of four fractions collected across the fractogram showed an increase in both size and fibril formation concurrent with increasing AsFlFFF elution times (Figure 5b). The change in the r_h to r_{rms} ratio as detected by MALS and QELS corroborated the presence of fibrils in the longer-retained fractions. These results support an emerging view that with protein aggregation diseases, smaller subfibrillar particles may be much more pathological than larger amyloid fibrils or plaques, which has implications on the development of therapies to treat these diseases.[40]

Drug and Gene Delivery. Size and size distributions are among the important parameters that govern drug and gene delivery efficiencies. AsFlFFF coupled with light scattering detectors is a characterization method for liposome preparations[53] and biodegradable *N*,*O*-dimethacryloylhydroxylamine (DMHA) cross-linked poly(*N*-isopropylmethacrylamide) (PNiPAM) thermosensitive nanogels that are being developed for use as drug delivery vehicles.[45] DMHA decomposes under physiologic conditions and has low *in vivo* toxicity. The size, molar mass, topology, particle number density, and byproducts from temperature and pH dependent erosion studies were monitored. At physiological conditions, the nanogel's weight average molecular weight decreased from 6×10^7 to 2×10^7 g mol^{-1} without a significant increase in size. A comparison of r_h to r_{rms} revealed that the nanogel topology remained constant despite extensive erosion, which was attributed to the self-cross-linking behavior of the PNiPAM. These observations substantiated an efficient design of a nanogel scaffolding for drug release.

FlFFF-MALS has monitored the size and stability of cationic surfactant-based non-viral vectors for gene therapy.[46] The addition of UV-vis and QELS detectors to AsFlFFF-MALS enabled the simultaneous measurement of composition and amount of free polycation and detection of aggregates in the final formulation of chitosan-based vectors, which subsequently allowed correlation with cell transfection rates.[47] The development of a gene delivery vehicle based on virus-like particles derived from the human polyoma JC-virus again reinforced the necessity of using a suite of detectors to obtain multiple levels of information.[41] These analyses provided insights into procedures and formulations essential for optimal stability and transfection rates and could not have been achieved without a separation stage.

Nanoparticle Toxicity. The potential risks of nanomaterials to human health and the environment have drawn a great deal of attention in the last several years. The National Nanotechnology Initiative held workshops and subsequently published documents that identify priority areas for environmental, health, and safety research needs for engineered nanoscale materials.[4] One key goal is the establishment of methods for nanoparticle

dx.doi.org/10.1021/ac101759z |*Anal. Chem.* 2011, 83, 634–642

quantification and characterization. This is particularly important because the physicochemical properties of nanomaterials vary substantially from batch-to-batch and vendor-to-vendor, which has led to inconsistent performance and behavior characteristics.

FlFFF with inductively coupled plasma MS (ICPMS) was used to study short term exposure toxicity of 2 and 5 nm CdSe/ZnS quantum dots (QD) with two different surface coatings, 11-mercaptoundecanoic acid (MUA) and polyethylene oxide (PEO).[27] The more stable PEO-QD were less acutely toxic to *Daphnia magna* than the MUA-QD, which is designed for accelerated dissolution. Dissolved Cd^{2+} was present in the MUA-QD suspension, and thus toxicity was attributed to cadmium poisoning. The PEO-QD suspension contained no dissolved Cd^{2+}, which indicated a different toxicity mechanism. The results of this study suggested that a small core size does not necessarily translate to greater toxicity and that the use of particle number or mass as a dose metric can lead to different conclusions.

INSTRUMENTAL ADVANCES

Developments in FFF instrumentation in the last decade have addressed nonideal behavior or extended FFF capabilities. The coupling of FFF with MALS-dRI, QELS, and MS has been beneficial to each technique. The train of more monodisperse samples eluting from the FFF channel alleviates the problem of selective detection and bias towards components that produce the strongest responses.[54] On the other hand, these detectors compensate for nonideal behavior, e.g., analyte-accumulation wall interactions that affect FFF retention times. Orthogonal techniques such as ICP MS, LC, and ESI MS provide a wealth of information and have opened gateways to nanoparticle toxicity and proteomic studies.[27,44] Some advances in FFF instrumentation and approaches are discussed below.

Online Concentration. Dilution is a common problem for elution-based separation methods. FFF separation takes place in the region near the accumulation wall, so the majority of the FFF channel is occupied by fluid only. Removal of fluid from the region furthest from the accumulation wall results in sample concentration. This has been accomplished by introducing a slot outlet positioned on the opposite channel surface to the accumulation wall at the detector end of the FFF channel.[55] Carrier liquid is continuously removed through the slot outlet leading to on-line sample concentration just prior to detection. A 14× increase in sample concentration has been demonstrated.[55,56]

Another useful approach for the analysis of dilute samples is the opposed flow sample concentration method.[57] A large volume of sample is introduced into the FlFFF channel, where it encounters an opposing flow. The ratio of the opposing flow rate to sample introduction flow rate determines the point along the FFF channel where sample is focused prior to the start of the separation. Because only particle-free fluid can exit through the semipermeable membrane accumulation wall, the sample is concentrated on the membrane. Sample volumes as large as 1 L have been loaded into a ~1.3 mL volume FlFFF channel, resulting in concentration factors as high as 10^5. However, depending on the flow rates used, sample loading can be time consuming. This approach was demonstrated in a symmetric FlFFF channel but can also be implemented in other FlFFF configurations.

High Throughput Separation. Parallel separations can increase sample throughput. This has been achieved by arranging multiple FlFFF channels in circular or parallel configurations.[44,58,59] Offline combination of 2D isoelectric focusing (IEF)-AsFlFFF[44] and multiplexed hollow fiber (MxHF5)-FlFFF[59] with nanoflow LC ESI MS/MS allowed profiling of urinary proteins and phospholipids in lipoproteins. IEF-AsFlFFF characterized human urinary proteins in less than 30 minutes. An IEF separation of the proteins by isoelectric point was followed by six multiplexed size-based AsFlFFF fractionations, each at a unique pH. Shotgun proteomics from each sample fraction identified 245 total and 110 novel proteins. The MxHF5-FlFFF experiments combined six hollow fiber channels in parallel for the semi-preparative sorting and collection of lipoproteins. The hollow fiber channel is disposable, which reduces cross-contamination risks of clinical samples.

Microchannels. Miniaturized channels have been introduced for many FFF systems such as ThFFF, AsFlFFF, and electrical FFF.[7,44,60] The reduction in channel dimensions offers advantageous features such as low sample consumption and shorter analysis times at lower energy and resource costs.

High Temperature and Nonaqueous FlFFF. A high temperature FlFFF instrument has been recently introduced for nonaqueous separations. Newly developed ceramic membranes stable at 130 °C and compatible with chlorinated organic solvents form the heart of the stainless steel channel that was used to fractionate semicrystalline ultrahigh *MW* polyethylene (PE).[35,36] High-temperature AsFlFFF combined with online IR, MALS, and viscometry detection identified and characterized the long chain branching component of low density PE.[36] This is critical to improved understanding of effects of long chain branching on the rheological and processing properties of polyolefins.[35,36] The pore size of the ceramic membrane determined the lower *MW* limit of 50 kDa. Continued membrane advancements such as smaller pore diameters and expanded solvent compatibility will open more doors for characterizing organosoluble macromolecules by FlFFF.

LOOKING TOWARDS THE FUTURE

FFF has come of age as a mainstream analytical technique for separating and characterizing analyte species that range in size from the low nanometers to tens of micrometers. The National Institute of Standards and Technology has used FFF to support the development of new certified reference materials. The Food and Drug Administration lists FFF among the common techniques used to characterize nanomaterials (Manual of Policies and Procedures 5015.9).

As the number of applications and publications rise, methods development is giving way to methods refinement, thereby making the implementation of FFF a less time consuming task for users new to the field. The number of potential FFF applications seems vast as new nanomaterials are designed and synthesized and new mixtures and hybrids are introduced. New challenges will arise as the applications of FFF instruments move beyond the instruments' original design purpose. An example is the FlFFF separation of <10 nm quantum dots suspended in organic solvents, for which suitable membranes are not currently commercially available. Moving from analytical scale to preparative scale applications is also a practical challenge. For example, typical FFF experiment sample injection volumes are tens of microliters containing ~10^6−10^8 nanoparticles. Though this provides good measurement statistics (relative to microscopy), this remains in the realm of analytical scale. Preparative scale separations that could produce suitable quantities of uniform samples for testing would greatly extend understanding of nano-sized material

properties and their relation to product performance. The time is also ripe for miniaturization because combined microfluidics and FFF knowledge could produce devices with improved diagnostic or online processing capabilities. Growing analytical needs that can be addressed by new applications of FFF-based instrumentation with different fields and capabilities will continue to drive development in this field.

BIOGRAPHIES

S. Kim R. Williams is an Associate Professor of Chemistry and the Director of the Laboratory for Advanced Separations Technologies at Colorado School of Mines. Research in the Williams lab focuses on the development and application of separation and characterization technologies for analytes that span nanometer to micrometer sizes. Dr. J. Ray Runyon is a postdoctoral researcher at the Colorado School of Mines. His research focuses on the development of novel FFF and light scattering approaches to characterize complex polymers and nanoparticles systems and ascertain structure-property-performance relationships. He received his Ph.D. in 2009 under the guidance of Prof. Williams. Akram Ashames is a Ph.D. graduate student in the Williams research group. With a B.Sc. in pharmacy from Alfateh University, Libya, his research focuses on developing and implementing FFF with different detection systems for the preparation and study of nanocarriers for drug delivery. Address correspondence to Williams at Laboratory for Advanced Separations Technologies, Department of Chemistry and Geochemistry, Colorado School of Mines, Golden, CO 80401; krwillia@mines.edu; Fax: 1-303-273-3629.

ACKNOWLEDGMENT

The authors gratefully acknowledge support from the National Science Foundation (CHE-0515521, CHE-1013029, CBET-0968042, and DMR-0820518). A. Ashames is supported by the Libyan Ministry of Education and Scientific Research.

REFERENCES

(1) Giddings, J. C. *Sep. Sci.* **1966**, *1*, 123–125.
(2) Giddings, J. C. *Science* **1993**, *260*, 1456–1465.
(3) Schimpf, M. E.; Caldwell, K. D.; Giddings, J. C. *Field-Flow Fractionation Handbook*; Wiley: New York, 2000.
(4) National Nanotechnology Initiative. http://www.nano.gov/NNI_EHS_Research_Strategy.pdf2008.
(5) Gascoyne, P. R. C. *Anal. Chem.* **2009**, *81*, 8878–8885.
(6) Williams, P. S.; Carpino, F.; Zborowski, M. *Mol. Pharmaceutics* **2009**, *6*, 1290–1306.
(7) Gale, B. K.; Caldwell, K. D.; Frazier, A. B. *Anal. Chem.* **2001**, *73*, 2345–2352.
(8) Semyonov, S. N.; Maslow, K. I. *J. Chromatogr. A* **1988**, *446*, 151–156.
(9) Myers, M. N.; Caldwell, K. D.; Giddings, J. C. *Sep. Sci.* **1974**, *9*, 47–70.
(10) Ratanathanawongs, S. K.; Shiundu, P. M.; Giddings, J. C. *Colloids Surf. A* **1995**, *105*, 243–250.
(11) Pasti, L.; Agnolet, S.; Dondi, F. *Anal. Chem.* **2007**, *79*, 5284–5296.
(12) Messaud, F. A.; Sanderson, R. D.; Runyon, J. R.; Otte, T.; Pasch, H.; Williams, S. K. R. *Prog. Polym. Sci.* **2009**, *34*, 351–368.
(13) Mes, E. P. C.; Kok, W. Th.; Tijssen, R. *Int. J. Polym. Anal. Charact.* **2003**, *8*, 133–153.
(14) Giddings, J. C.; Yang, F. J. F.; Myers, M. N. *Anal. Chem.* **1974**, *46*, 1917–1924.
(15) Barman, B. N.; Giddings, J. C. *Langmuir* **1992**, *8*, 51–58.
(16) Beckett, R.; Ho, J.; Jiang, Y.; Giddings, J. C. *Langmuir* **1991**, *7*, 2040–2047.
(17) Fromell, K.; Hulting, G.; Ilichev, A.; Larsson, A.; Caldwell, K. D. *Anal. Chem.* **2007**, *79*, 8601–8607.
(18) Giddings, J. C.; Yang, F. J.; Myers, M. N. *Anal. Chem.* **1976**, *48*, 1126–1132.
(19) Davis, J. M. *Anal. Chim. Acta* **1991**, *246*, 161–169.
(20) Wahlund, K. G.; Giddings, J. C. *Anal. Chem.* **1987**, *59*, 1332–1339.
(21) Zattoni, A.; Rambaldi, D. C.; Roda, B.; Parisi, D.; Roda, A.; Moon, M. H.; Reschiglian, P. *J. Chromatogr. A* **2008**, *1183*, 135–142.
(22) Gascoyne, P. R. C.; Noshari, J.; Anderson, T. J.; Becker, F. F. *Electrophoresis* **2009**, *30*, 1388–1398.
(23) Peng, H.; Alvarez, N. T.; Kittrell, C.; Hauge, R. H.; Schmidt, H. K. *J. Am. Chem. Soc.* **2006**, *128*, 8396–8397.
(24) Arfvidsson, C.; Wahlund, K. G. *Anal. Biochem.* **2003**, *313* 76–85.
(25) Rameshwar, T.; Samal, S.; Lee, S.; Kim, S.; Cho, J.; Kim, I. S. *J. Nanosci. Nanotechnol.* **2006**, *6*, 2461–2467.
(26) Lee, D.; Williams, S. K. R. *J. Chromatogr. A* **2010**, *1217*, 1667–1673.
(27) Pace, H. E.; Lesher, E. K.; Ranville, J. F. *Environ. Toxicol. Chem.* **2010**, *29*, 1338–1344.
(28) Zattoni, A.; Rambaldi, D. C.; Reschiglian, P.; Melucci, M.; Krol, S.; Garcia, A. M. C.; Sanz-Medel, A.; Roessner, D.; Johann, C. *J. Chromatogr. A* **2009**, *1216*, 9106–9112.
(29) Kato, H.; Nakamura, A.; Takahashi, K.; Kinugasa, S. *Phys. Chem. Chem. Phys.* **2009**, *11*, 4946–4948.
(30) Chun, J.; Fagan, J. A.; Hobbie, E. K.; Bauer, B. J. *Anal. Chem.* **2008**, *80*, 2514–2523.
(31) Jackson, B. P.; Ranville, J. F.; Bertsch, P. M.; Sowder, A. G. *Environ. Sci. Technol.* **2005**, *39*, 2478–2485.
(32) Krachler, R.; Krachler, R. F.; von der Kammer, F.; Süphandag, A.; Jirsa, F.; Ayromlou, S.; Hofmann, T.; Keppler, B. K. *Sci. Total Environ.* **2010**, *408*, 2402–2408.
(33) Baalousha, M.; Lead, J. R. *Environ. Sci. Technol.* **2007**, *41*, 1111–1117.
(34) Rolland-Sabaté, A.; Colonna, P.; Mendez-Montealvo, M. G.; Planchot, V. *Biomacromolecules* **2007**, *8*, 2520–2532.
(35) Otte, T.; Brüll, R.; Macko, T.; Pasch, H.; Klein, T. *J. Chromatogr. A* **2010**, *1217*, 722–730.
(36) Mes, E. P. C.; de Jonge, H.; Klein, T.; Welz, R. R.; Gillespie, D. T. *J. Chromatogr. A* **2007**, *1154*, 319–330.
(37) Yohannes, G.; Shan, J.; Jussila, M.; Nuopponen, M.; Tenhu, H.; Riekkola, M. L. *J. Sep. Sci.* **2005**, *28*, 435–442.
(38) Demeule, B.; Lawrence, M. J.; Drake, A. F.; Gurny, R.; Arvinte, T. *Biochim. Biophys. Acta* **2007**, *1774*, 146–153.
(39) Cao, S.; Pollastrini, J.; Jiang, Y. *Curr. Pharm. Biotechnol.* **2009**, *10*, 382–390.
(40) Silveira, J. R.; Raymond, G. J.; Hughson, A. G.; Race, R. E.; Sim, V. L.; Hayes, S. F.; Caughey, B. *Nature* **2005**, *437*, 257–261.
(41) Citkowicz, A.; Petry, H.; Harkins, R. N.; Ast, O.; Cashion, L.; Goldmann, C.; Bringmann, P.; Plummer, K.; Larsen, B. R. *Anal. Biochem.* **2008**, *376*, 163–172.
(42) Lipin, D. I.; Lua, L. H. L.; Middelberg, A. P. J. *J. Chromatogr. A* **2008**, *1190*, 204–214.
(43) Chuan, Y. P.; Fan, Y. Y.; Lua, L.; Middelberg, A. P. J. *Biotechnol. Bioeng.* **2008**, *99*, 1425–1433.
(44) Kim, K. H.; Moon, M. H. *J. Proteome Res.* **2009**, *8*, 4272–4278.
(45) Smith, M. H.; South, A. B.; Gaulding, J. C.; Lyon, L. A. *Anal. Chem.* **2009**, *82*, 523–530.
(46) Lee, H.; Williams, S. K. R.; Allison, S. D.; Anchordoquy, T. J. *Anal. Chem.* **2001**, *73*, 837–843.
(47) Ma, P. L.; Buschmann, M. D.; Winnik, F. M. *Biomacromolecules* **2010**, *11*, 549–554.
(48) Runyon, J. R.; Goering, A.; Williams, S. K. R.; Yong, K. Pittsburgh Conference on Analytical Chemistry and Applied Spectroscopy, Chicago, 2009, Abstract 590-14.

(49) Schimpf, M. E.; Wheeler, L. M.; Romeo, P. F. In *ACS Symposium Series 521*, Provder, T., Ed.; ACS Publications: Washington, DC, 1993; pp 63−76.
(50) Rosenberg, A. S. *AAPS J.* **2006**, *8*, No. E501-E507.
(51) Carpenter, J. F.; Randolph, T. W.; Jiskoot, W.; Crommelin, D. J. A.; Middaugh, C. R.; Winter, G.; Fan, Y. X.; Kirshner, S.; Verthelyi, D.; Kozlowski, S.; Clouse, K. A.; Swann, P. G.; Rosenberg, A.; Cherney, B. *J. Pharm. Sci.* **2009**, *98*, 1201–1205.
(52) Singh, S. K.; Afonina, N.; Awwad, M.; Bechtold-Peters, K.; Blue, J. T.; Chou, D.; Cromwell, M.; Krause, H.-J.; Mahler, H.-C.; Meyer, B. K.; Narhi, L.; Nesta, D. P.; Spitznagel, T. *J. Pharm. Sci.* **2010**, *99*, 3302–3321.
(53) Hupfeld, S.; Moen, H. H.; Ausbacher, D.; Haas, H.; Brandl, M. *Chem. Phys. Lipids* **2010**, *163*, 141–147.
(54) Kassalainen, G. E.; Williams, S. K. R. *Anal. Chem.* 2003, *75*, 1887–1894.
(55) Prestel, H.; Niessner, R.; Panne, U. *Anal. Chem.* **2006**, *78*, 6664–6669.
(56) Leeman, M.; Islam, M. T.; Haseltine, W. G. *J. Chromatogr. A* **2007**, *1172*, 194–203.
(57) Lee, H.; Williams, S. K. R.; Giddings, J. C. *Anal. Chem.* **1998**, *70*, 2495–2503.
(58) Maskos, M.; Schupp, W. *Anal. Chem.* **2003**, *75*, 6105–6108.
(59) Lee, J. Y.; Min, H. K.; Choi, D.; Moon, M. H. *J. Chromatogr. A* **2010**, *1217*, 1660–1666.
(60) Janca, J. *Microthermal field-flow fractionation: analysis of synthetic, natural, and biological macromolecules and particles*; HBN Publishing: New York, 2008.